Electronic Supplementary Material (ESI) for Physical Chemistry Chemical Physics.
This journal is © the Owner Societies 2014

Supporting Information for:

Pentaglyme-K Salts Binary Mixtures: Phase Behavior, Solvate Structures, and Physicochemical Properties

Toshihiko Mandai,[†,I,*] *Seiji Tsuzuki,*[‡] *Kazuhide Ueno,*[†] *Kaoru Dokko,*[†,§] *and Masayoshi Watanabe*[†,*]

[†]Department of Chemistry and Biotechnology, Yokohama National University,

79-5 Tokiwadai, Hodogaya-ku, Yokohama 240-8501, Japan

[‡] National Institute of Advanced Industrial Science and Technology (AIST),

Tsukuba Central 2, Tsukuba, Ibaraki 305-8568, Japan

[§]Unit of Elements Strategy Initiative for Catalysts & Batteries (ESICB), Kyoto University,

Kyoto 615-8510, Japan

[I]Department of Applied Physics, Chalmers University of Technology,

Göteborg, SE-412 96, Sweden

We summarize the complete analytical data for a series of $[K(G5)_n]X$. DSC and TG curves of $[K(G5)_n]X$ with $[TFSA]^-$, $[TfO]^-$, $[NfO]^-$, PF_6^-, and SCN^- anions are shown in **Figures S1** and **S3**. Optimized structures of a series of parent K salts are displayed in **Figure S2**. Selected torsion angles and selected K–O_{glyme} distances of the solved structures in the crystalline state are listed in **Tables S2** and **S3**, respectively. Thermal ellipsoid model of $[K(G5)_1][TfO]$ is displayed in **Figure S4**. Crystallographic data (**Table S1**), solvate structures (**Figures S5–S7**), anionic Raman spectra (**Figure S8**), and selected vibrational frequencies (**Table S4**) of $[K(18C6)_1]X$ are also included below. In addition, Raman spectra for $[K(G5)_2]PF_6$ is attached in **Figure S9**. Temperature dependences of density, concentration, viscosity, and ionic conductivity for $[K(G5)_1][TFSA]$, $[K(G5)_1][NfO]$, and $[K(G5)_1]SCN$ are also included in **Figures S10** and **S11**.

Table S1. Crystallographic data of $[K(G5)_1][TfO]$, $[K(18C6)_1][TfO]$, $[K(18C6)_1]PF_6$, and $[K(18C6)_1]SCN$.

	$[K(G5)_1][TfO]$	$[K(18C6)_1][TfO]$	$[K(18C6)_1]PF_6$	$[K(18C6)_1]SCN$
Chemical formula	$C_{13}H_{26}F_3KO_9S$	$C_{13}H_{24}F_3KO_9S$	$C_{12}H_{24}F_6KO_6P$	$C_{13}H_{24}K_1N_1O_6S_1$
Formula weight	454.50	344.72	388.77	361.49
Crystal system	Orthorhombic	Monoclinic	Orthorhombic	Monoclinic
Space group	*Pbca*	$P2_1/n$	*Pnn*2	$P2_1/c$
a / Å	16.209(3)	8.6188(6)	7.840(3)	8.182(3)
b / Å	15.443(3)	16.5613(10)	10.813(5)	14.222(4)
c / Å	16.537(2)	14.2025(11)	11.426(5)	7.709(3)
α / º	90	90	90	90
β / º	90	95.439(4)	90	98.717(5)
γ / º	90	90	90	90
V / Å^3	4139.5(11)	2018.1(3)	968.7(7)	886.8(5)
Z	8	4	2	2
D_{calc} / g cm^{-3}	1.448	1.489	1.537	1.354
μ / mm^{-1}	0.4242	0.4348	0.4372	0.442
Temp. / ºC	−100	−100	−100	−100
Reflections collected	30178	15495	7086	6828
Independent reflection, R_{int}	4730, 0.0469	4629, 0.0376	2192, 0.0442	2023, 0.0446
R_1 [$I > 2\sigma(I)$]	0.0534	0.0798	0.0540	0.0473
wR_2 (all data)	0.1354	0.2249	0.1643	0.1252
GooF	1.149	1.073	1.060	1.125

Table S2. Selected torsion angles of the coordinating glymes for $[K(G5)_1][TFSA]$, $[K(G5)_1][TfO]$, and $[K(G5)_1]PF_6$ solvates. For $[K(G5)_1][TFSA]$, the angles of the octa-coordinated solvate were listed. Atomic numbering is corresponding to the numbering in each crystallographic data.

Selected angles / º	$[K(G5)_1][TFSA]$	$[K(G5)_1][TfO]$	$[K(G5)_1]PF_6$
C1−O1−C2−C3	−176.3(4)	−179.18(17)	170.4(2)
O1−C2−C3−O2	64.9(5)	64.7(3)	-62.8(3)
C2−C3−O2−C4	167.8(3)	174.47(15)	−171.43(19)
C3−O2−C4−C5	174.3(3)	−175.76(15)	−174.70(19)
O2−C4−C5−O3	−68.6(5)	-68.5(3)	71.4(3)
C4−C5−O3−C6	−178.5(4)	−179.82(16)	−179.81(17)
C5−O3−C6−C7	171.7(4)	175.12(16)	−174.33(17)
O3−C6−C7−O4	64.5(6)	64.8(3)	-65.3(3)
C6−C7−O4−C8	−176.8(4)	175.44(16)	−172.68(17)
C7−O4−C8−C9	175.2(4)	−179.44(16)	178.91(18)
O4−C8−C9−O5	−69.3(5)	−69.8(3)	69.7(3)
C8−C9−O5−C10	−174.0(3)	174.31(15)	175.28(17)
C9−O5−C10−C11	172.0(3)	170.92(16)	−178.63(17)
O5−C10−C11−O6	70.2(4)	62.5(3)	−69.2(3)
C10−C11−O6−C12	−173.9(3)	−172.55(18)	176.59(19)

Table S3. Distances between K^+ cation and oxygen atoms of the coordinating glymes for $[K(G5)_1][TFSA]$, $[K(G5)_1][TfO]$, and $[K(G5)_1]PF_6$ solvates. For $[K(G5)_1][TFSA]$, the distances of the octa-coordinated solvate were listed. Atomic numbering is corresponding to the numbering in each crystallographic data.

Distances / Å	$[K(G5)_1][TFSA]$	$[K(G5)_1][TfO]$	$[K(G5)_1]PF_6$
K1−O1	2.850(4)	2.8887(18)	2.8201(19)
K1−O2	2.850(4)	2.8531(17)	2.9100(19)
K1−O3	2.855(3)	2.8817(16)	2.8648(18)
K1−O4	2.906(4)	2.8584(16)	2.8322(17)
K1−O5	2.826(4)	2.9427(17)	2.8807(18)
K1−O6	2.913(3)	2.8888(17)	2.9069(19)

Table S4. Selected vibrational frequencies of the coordinating glymes and counter anions observed in the measured Raman spectra for $[K(18C6)_1]X$ at ambient temperature.

	Raman shift / cm^{-1}				
	$[K(18C6)_1][TFSA]$	$[K(18C6)_1][TfO]$	$[K(18C6)_1][NfO]$	$[K(18C6)_1]PF_6$	$[K(18C6)_1]SCN$
Complex cation	870	871	873	874	870
	833	831	834	835	834
Counter anions	742	1033	1024	743	735

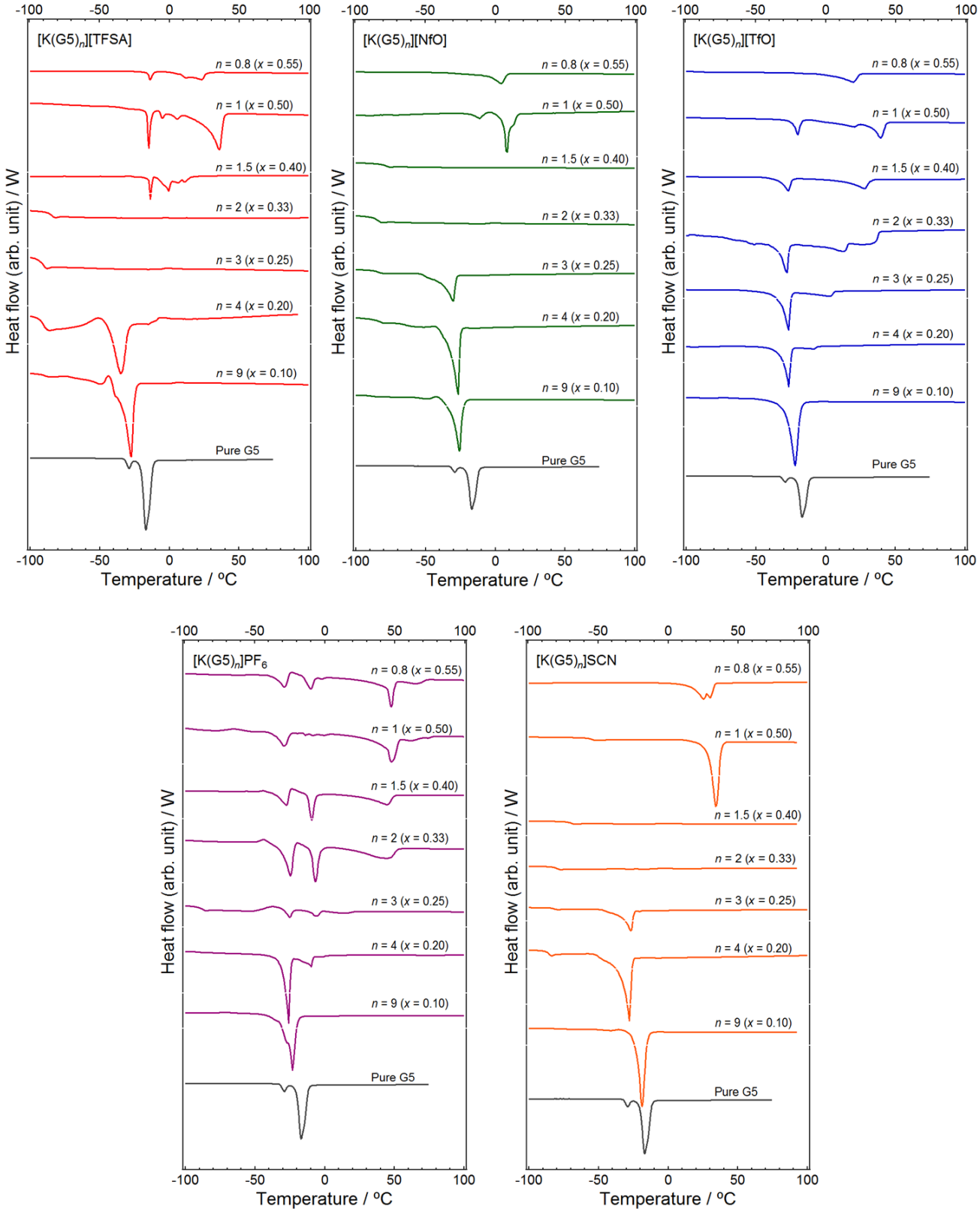

Figure S1. DSC curves of $[K(G5)_n]X$ with $[TFSA]^-$, $[TfO]^-$, $[NfO]^-$, PF_6^-, and SCN^- anions.

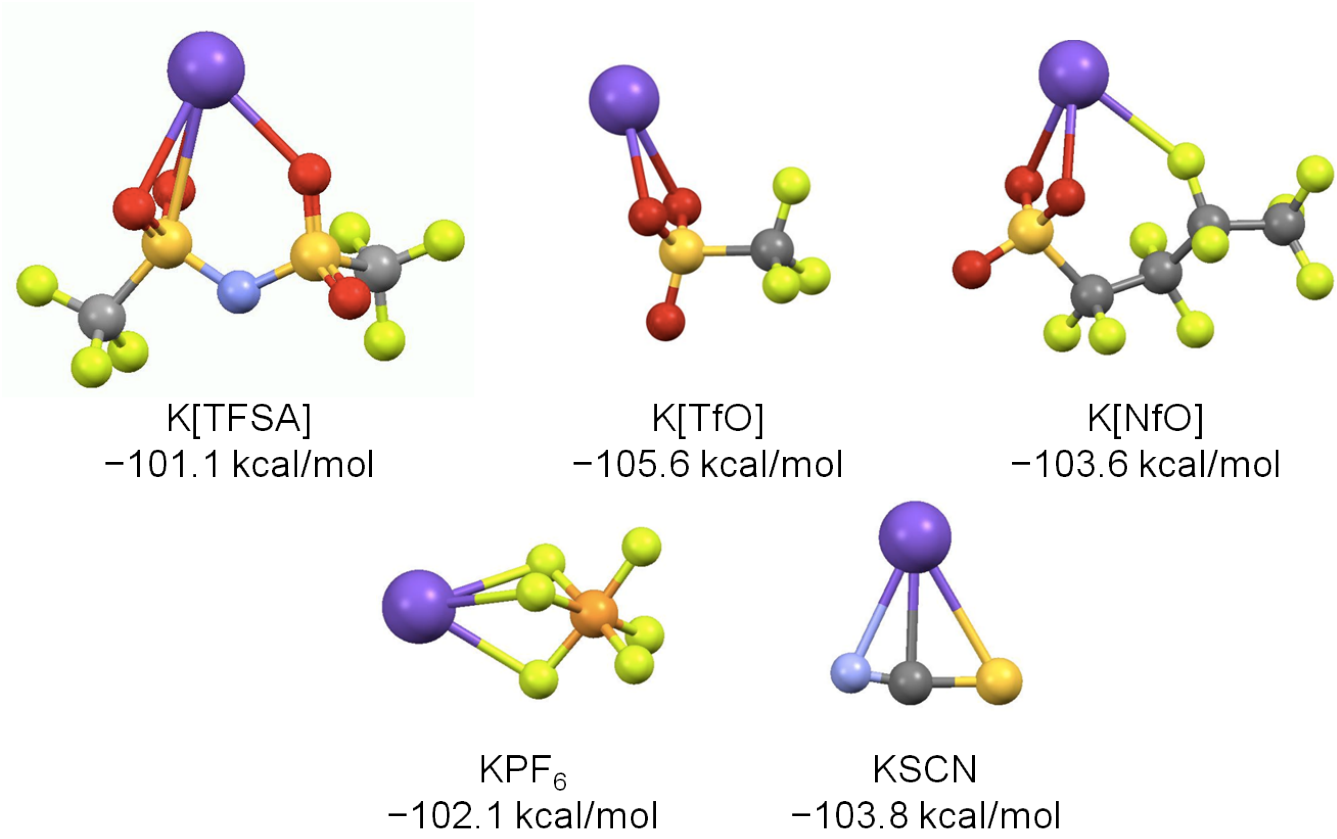

Figure S2. Optimized structures of a series of parent K-salts calculated by *ab initio* quantum calculation.

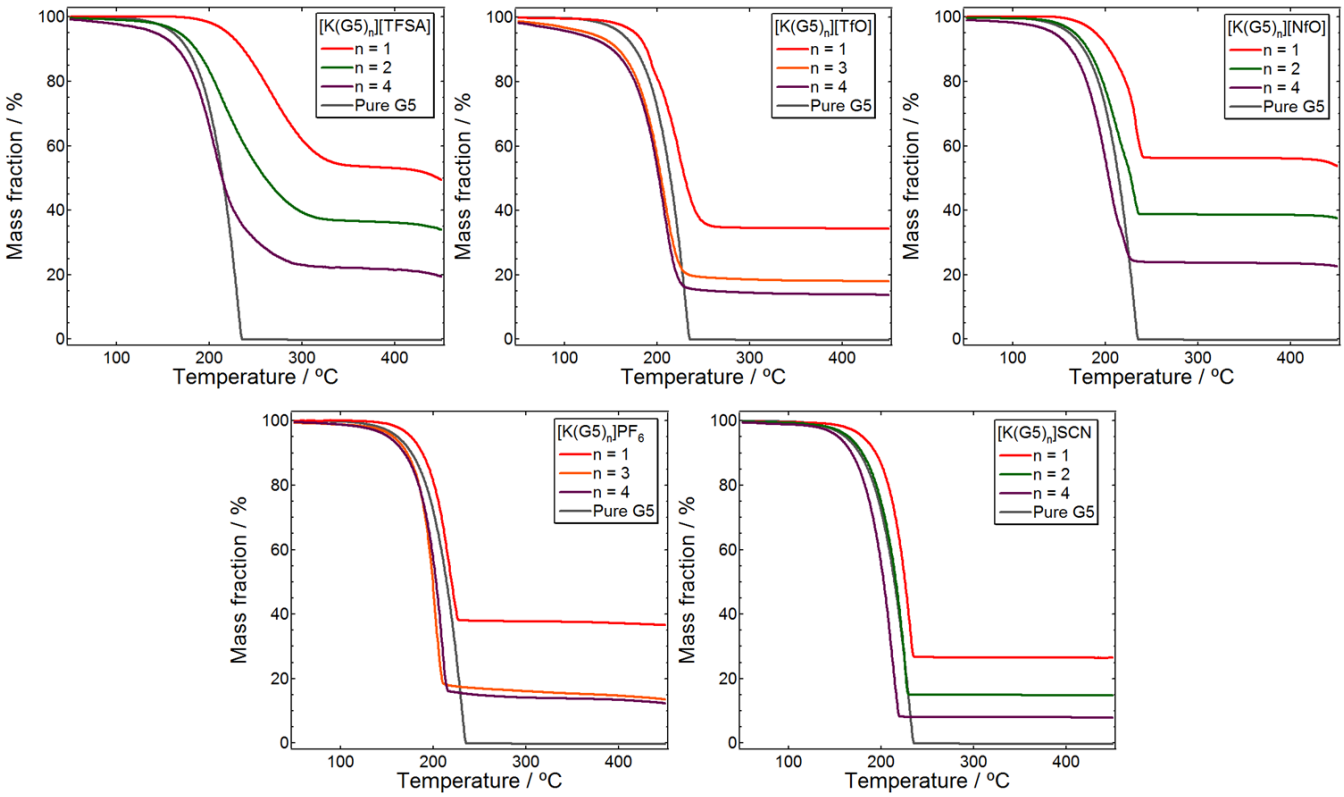

Figure S3. TG curves of the selected [K(G5)$_n$]X paired with [TFSA]$^-$, [TfO]$^-$, [NfO]$^-$, PF_6^-, and SCN^- anions. The curves of Pure G5 was also included in each figure.

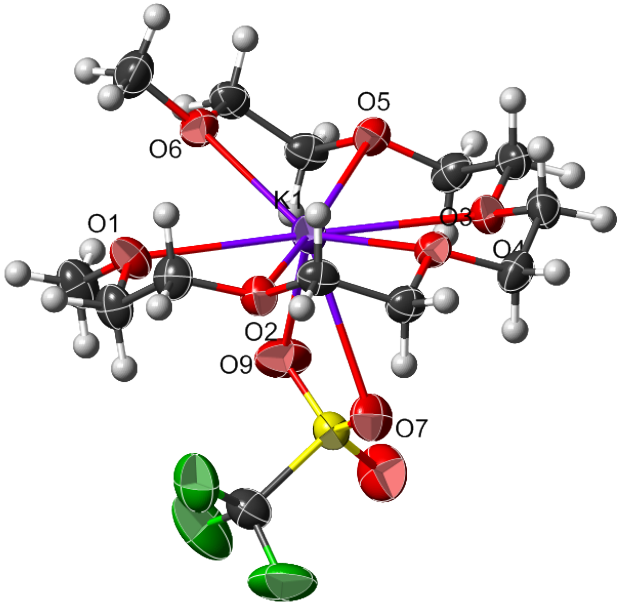

Figure S4. Thermal ellipsoid model of $[K(G5)_1][TfO]$. The ellipsoids of non-hydrogen atoms are drawn at the 50 % probability level while isotropic hydrogen atoms are represented by spheres of arbitrary size. The labels of uncoordinating atoms are omitted for clarity. CCDC: 1030104.

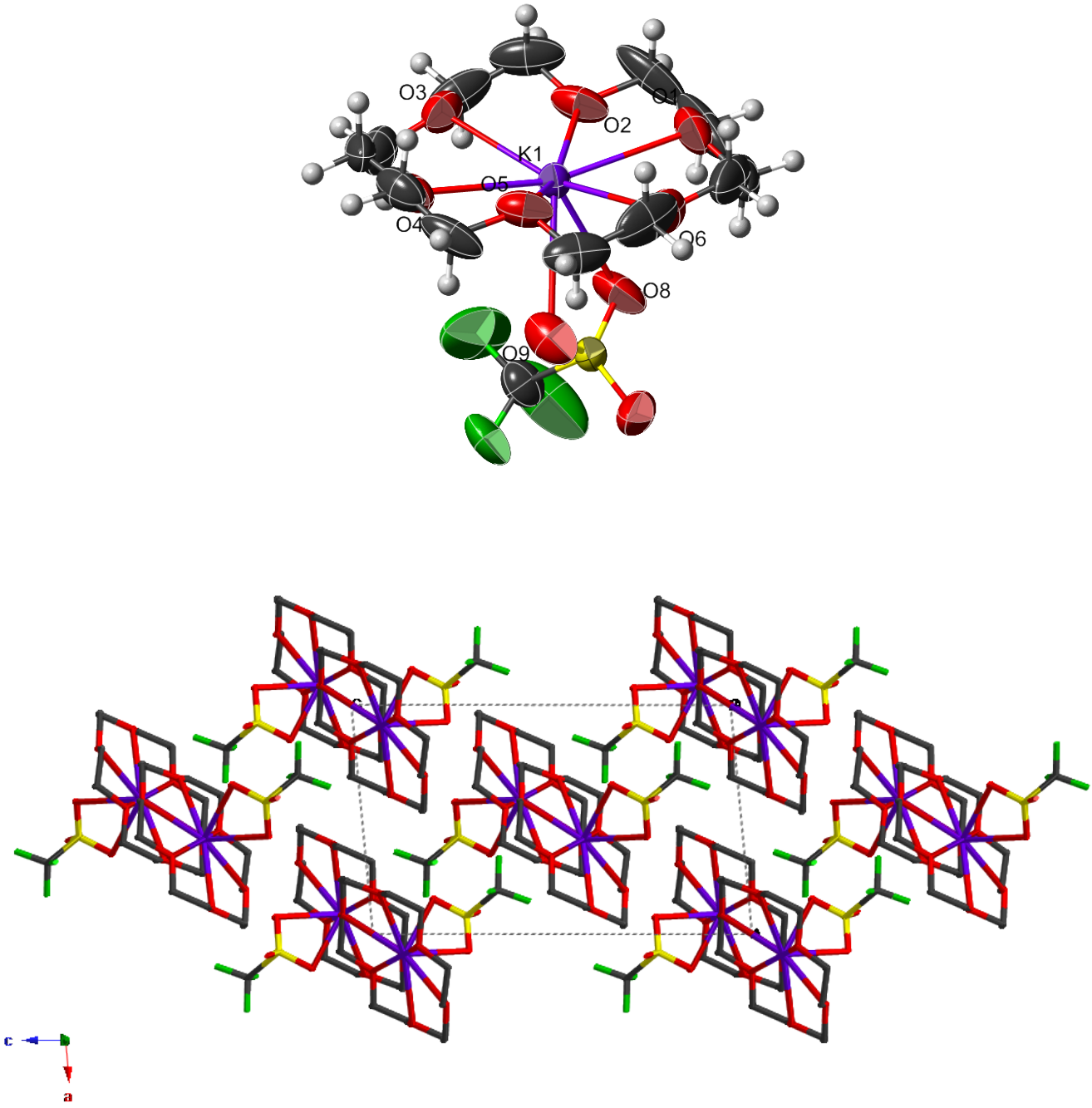

Figure S5. Thermal ellipsoid model (upper) and packing structure along *b*-axis (lower) of $[K(18C6)_1][TfO]$. The ellipsoids of non-hydrogen atoms are drawn at the 50 % probability level while isotropic hydrogen atoms are represented by spheres of arbitrary size. The labels of uncoordinating atoms are omitted for clarity. CCDC: 1030105.

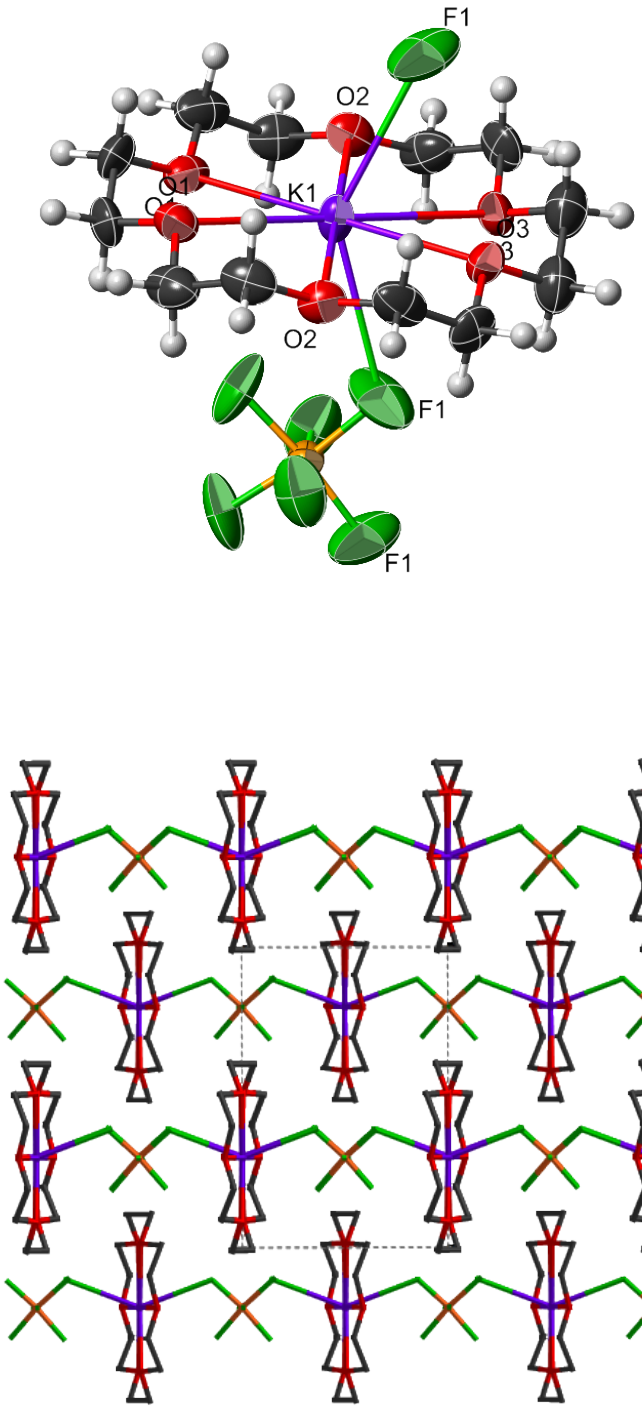

Figure S6. Thermal ellipsoid model (upper) and packing structure along *b*-axis (lower) of $[K(18C6)_1]PF_6$. The ellipsoids of non-hydrogen atoms are drawn at the 50 % probability level while isotropic hydrogen atoms are represented by spheres of arbitrary size. The disordered atoms and labels of uncoordinating atoms are omitted for clarity. The expanded structure is shown here. CCDC: 1030106.

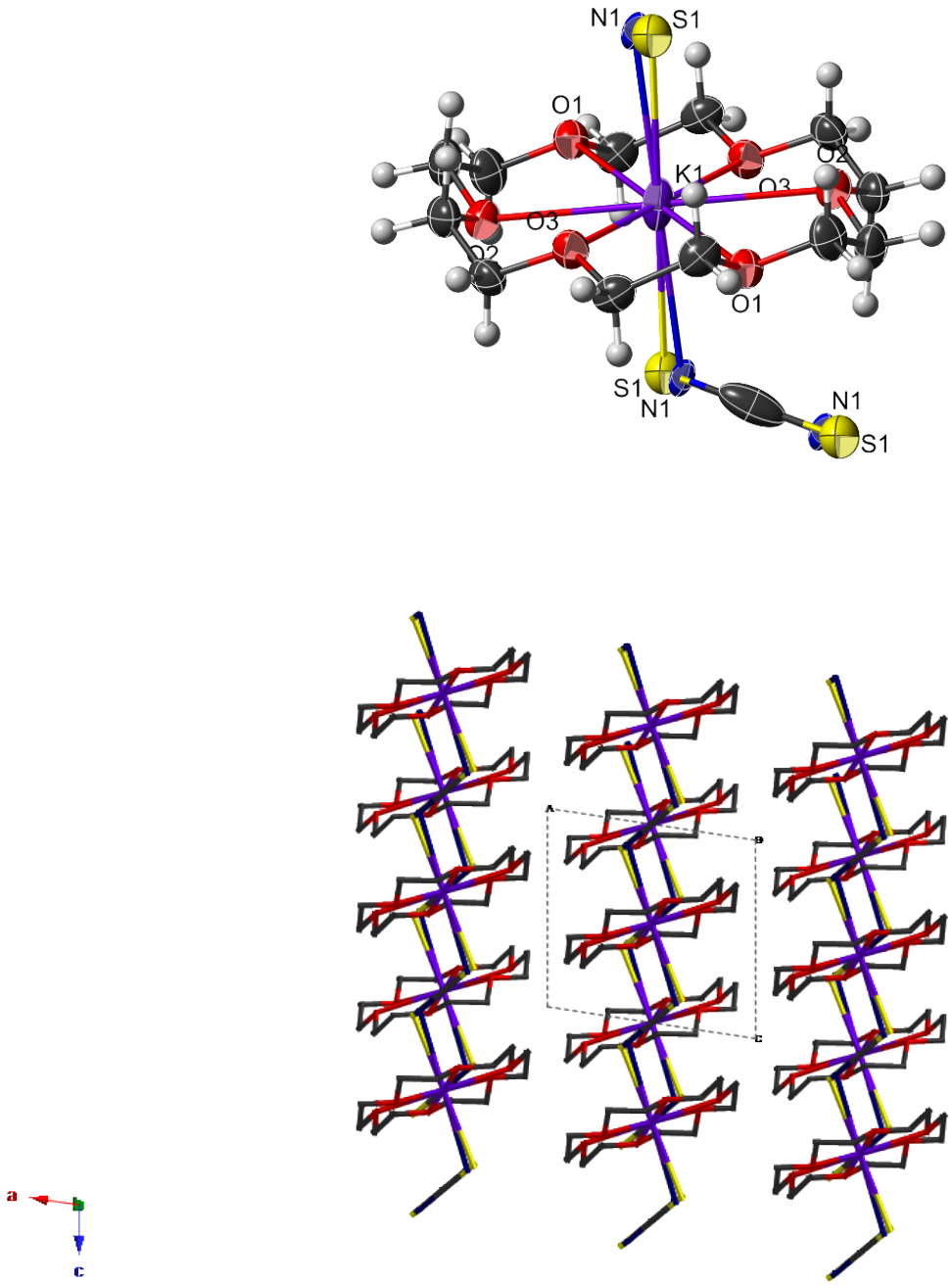

Figure S7. Thermal ellipsoid model (upper) and packing structure along *b*-axis (lower) of $[K(18C6)_1]SCN$. The ellipsoids of non-hydrogen atoms are drawn at the 50 % probability level while isotropic hydrogen atoms are represented by spheres of arbitrary size. The labels of uncoordinating atoms are omitted for clarity. The expanded structure is shown here. CCDC: 1030107.

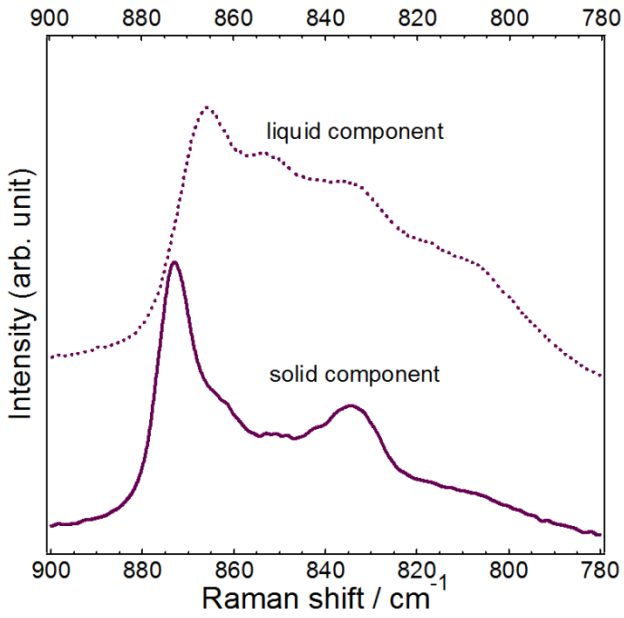

Figure S8. Raman spectra of the precipitated solid and supernatant liquid components for $[K(G5)_2]PF_6$ in the range of 900–780 cm^{-1} at ambient temperature.

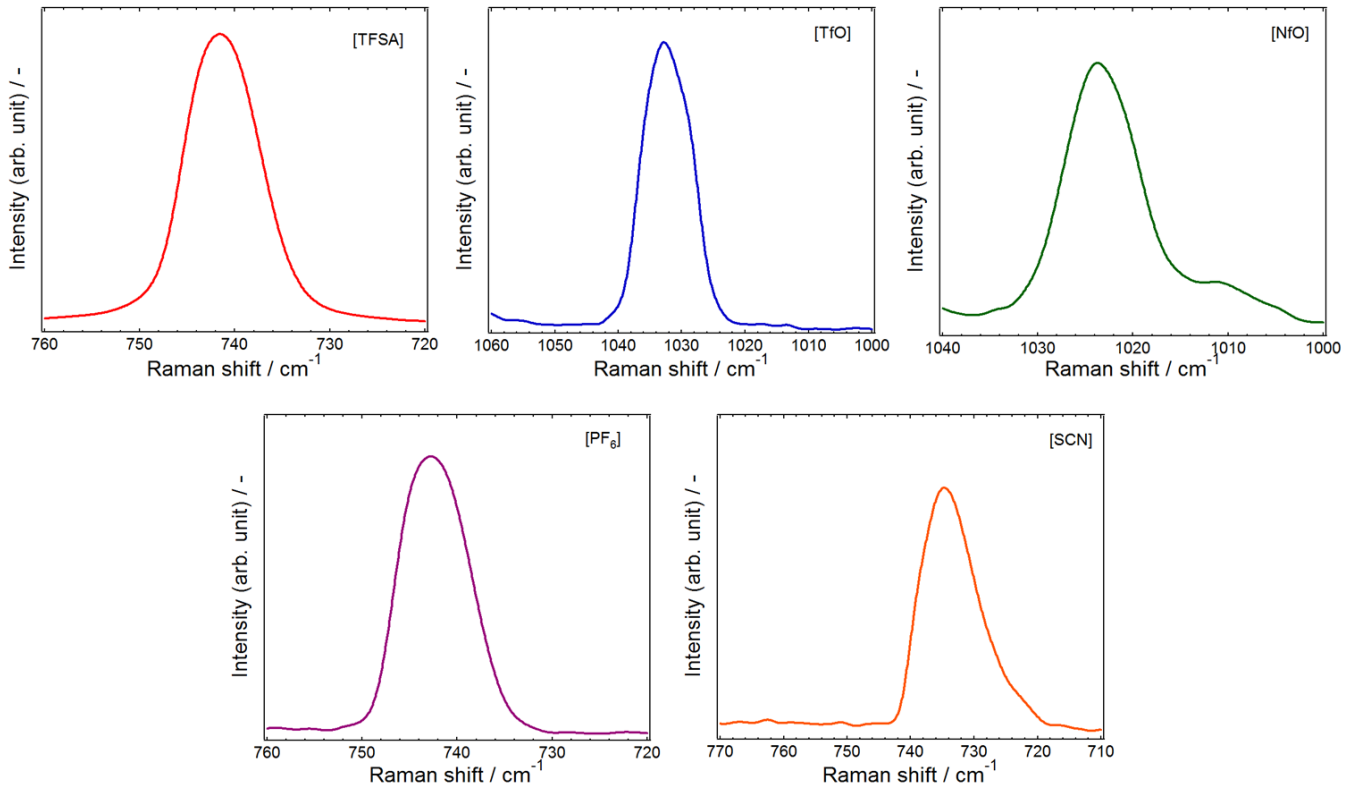

Figure S9. Anionic Raman spectra for $[K(18C6)_1][TFSA]$, $[K(18C6)_1][TfO]$, $[K(18C6)_1][NfO]$, $[K(18C6)_1]PF_6$, and $[K(18C6)_1]SCN$ in the crystalline state measured at ambient temperature.

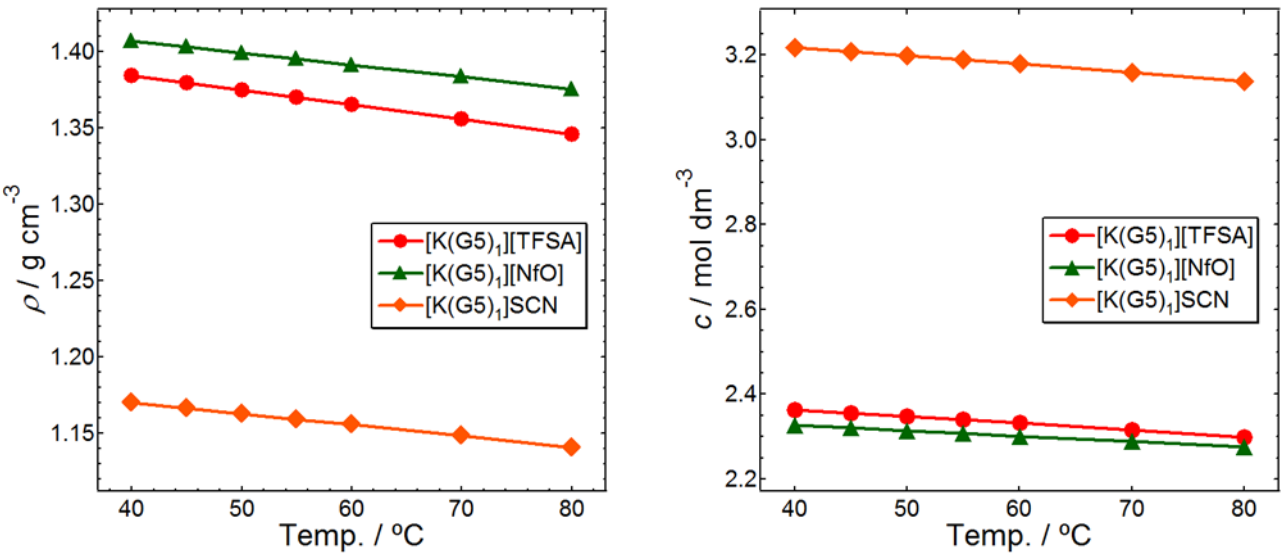

Figure S10. Temperature dependences of the density (left) and concentration (right) for $[K(G5)_1][TFSA]$, $[K(G5)_1][NfO]$, and $[K(G5)_1]SCN$.

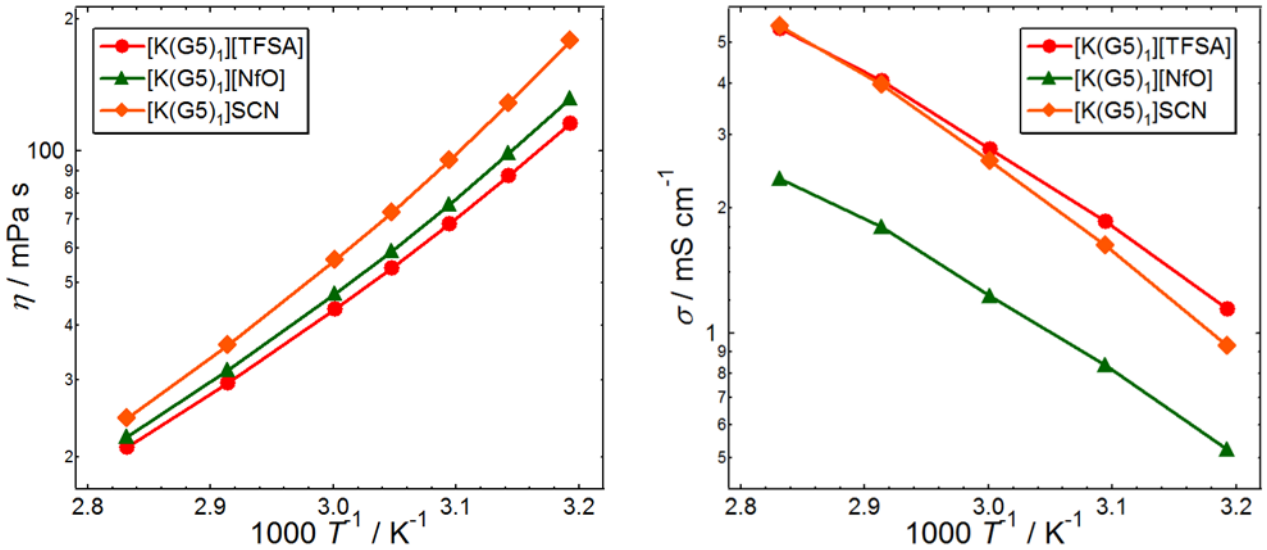

Figure S11. Temperature dependences of the viscosity (left) and ionic conductivity (right) for $[K(G5)_1][TFSA]$, $[K(G5)_1][NfO]$, and $[K(G5)_1]SCN$.